Mode Charts for Magnetized Ferrite Cylinders

CHRISTIAN SCHIEBLICH

Abstract—**Waveguide junction circulators in E- and H-plane technique usually employ height-dependent ferrite modes. The most crucial parameter is the frequency splitting between two angle-dependent modes. It rises with the magnetic bias field until there is a maximum at about saturation. In this contribution, mode charts are given which help the designer to look up the resonance frequencies of the most important modes as a function of the external, measurable field. Also, the unsaturated state of the ferrite material is covered. These diagrams are in good accordance with experimental experience and have been helpful in interpreting circulator performance, especially for the identification of spurious resonances.**

I. Introduction

JUNCTION circulators are based on the splitting of an angle-dependent resonator mode in a ferrite cylinder by a magnetic bias field. To determine the resonator dimensions, mode charts are helpful. They should also give information about the shift and splitting of the resonance frequencies versus bias field.

Mode charts have been published for cylinders with height-independent modes and magnetically conducting edge [1], and they are a good approximation for the ferrites in stripline circulators. In [2], Helszajn and Sharp use the magnetic wall model also for height-dependent modes of magnetized ferrite cylinders. For an open flat face of the ferrite, the magnetic wall assumption is replaced by a more refined model. In [3], the same authors treat the EH_{11} resonance of a composite ferrite/dielectric structure without assuming a magnetic azimuthal wall, but only in the isotropic case. As early as 1967, Godtmann and Haas [4], [5] published mode charts for a magnetized ferrite cylinder between two metallic plates by an exact modal analysis, also without the magnetic wall assumption. They do not cover, however, the case of nonsaturated ferrites. An infinite bias field is taken as an isotropic limit, and the resonant frequencies are traced when reducing it until maximum frequency splitting is reached at zero field. In reality, however, the completely demagnetized ferrite is also isotropic, and there is a maximum splitting between zero and infinite bias field. This is found just in the transition region between the unsaturated and the saturated state. Because sensitivity of the frequency splitting to bias field variations (e.g., caused by temperature variations) is also low at this maximum, this is the preferred operating point for junction circulators.

For practical reasons, it is more appropriate to trace the resonance frequencies with the bias field rising from zero towards saturation. The infinite bias field, which is taken in [4] and [5] as an isotropic limit, is only of academic interest. Hauth [6], [7] has analyzed some rather general open structures including the unsaturated state. His rigorous analysis can be used to analyze the ferrite in its specific environment, and it is not the intent of this paper to replace such rigorous calculations. The mode charts given here are only to help the designer in finding suitable ferrite dimensions and the achievable frequency splitting, as well as the frequencies of neighboring modes.

II. Microwave Permeability of Magnetized Ferrites

The elements of the permeability tensor (bias field in the z direction),

$$\vec{\mu} = \begin{pmatrix} \mu & -j\kappa & 0 \\ j\kappa & \mu & 0 \\ 0 & 0 & \mu_z \end{pmatrix} \mu_0 \tag{1}$$

above saturation are given by the classical theory of Polder [8], while for the unsaturated state usually the empirical formulas of Green and Sandy [9] are used. Unfortunately these two descriptions do not join continuously, so that the practically important transient region is not correctly described. Hansson and Filipsson [10] give formulas for the whole range of bias fields, with even the derivatives of the tensor elements being continuous:

$$\mu = \mu_e + (1-\mu_e)m^{3/2} + \frac{h_i}{h_i^2 - w^2}$$

$$\kappa = -\frac{mw}{h_i^2 - w^2} \qquad \mu_z = \mu_e^{(1-m^{5/2})} \tag{2}$$

with the normalized values

$$h_i = \frac{H_i}{M_s} \qquad m = \frac{M}{M_s}$$

$$w = \frac{\omega}{\omega_m} > 1 \qquad \omega_m = -\gamma\mu_0 M_s$$

$$\mu_e = \frac{1}{3}\left(1 + 2\sqrt{1 - \frac{1}{w^2}}\right).$$

M_s is the saturation magnetization, M the actual magneti-

Manuscript received November 30, 1988; revised April 25, 1989. This work was supported by the Deutsche Forschungsgemeinschaft.

The author was with the Arbeitsbereich Hochfrequenztechnik, Technische Universität Hamburg-Harburg, D-2100 Hamburg 90, West Germany. He is now with the CERN European Research Center, CH-1211 Geneva 23, Switzerland.

IEEE Log Number 8929888.

0018-9480/89/1000-1555$01.00 ©1989 IEEE

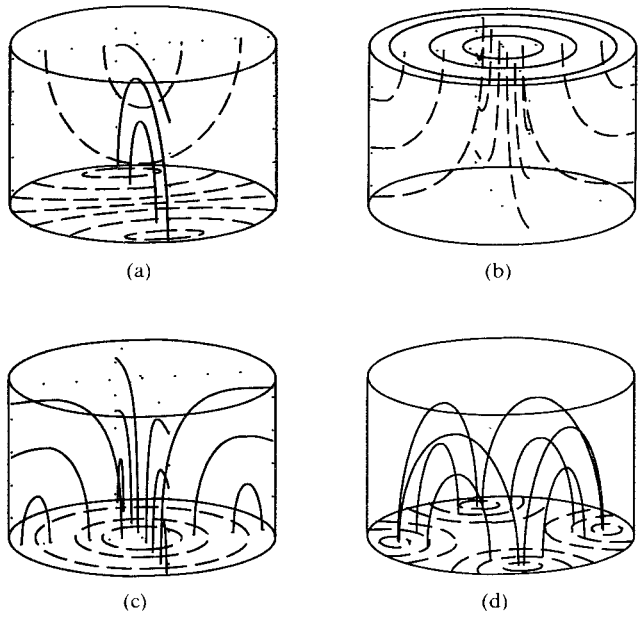

Fig. 1. Some resonator modes of the dielectric cylinder (bottom electric wall, top magnetic wall; ——— electric field, – – – – magnetic field): (a) $EH_{11(1/2)}$, (b) $H_{01(1/2)}$, (c) $E_{01(1/2)}$, (d) $EH_{21(1/2)}$.

zation, H_i the internal magnetic bias field, and γ the (negative) gyromagnetic ratio.

The external field H_a is partitioned into the inner field and the magnetization (flat disk, demagnetization factor 1). The ratio depends on the static magnetization characteristics of the material. In [10] it is given as

$$H_a = M + H_i$$

$$H_i = 0 \qquad \text{for } M < M_r = a_1 M_s$$

$$M = M_r + (M_s - M_r)\left(\coth(a_2 H_i) - \frac{1}{a_2 H_i}\right). \tag{3}$$

M_r is approximately the remanence magnetization. The form factors a_1 and a_2 are tabulated in [10] for common ferrite materials; their values are approximately $a_1 \approx 0.6$, and $a_2 \approx 8$ $(\mathrm{A/m})^{-1}$. These values have been used for the following calculations.

III. Resonance Frequencies in the Isotropic Case

The ferrite will be treated as a piece of dielectric waveguide terminated by electric or magnetic walls at its end surfaces. To a first approximation, the lateral wall can be assumed as a perfect magnetic conductor; the eigenwaves are then purely E (TM) or H (TE). Without assuming the boundary as a magnetic wall, these modes, except those with $m = 0$, become the hybrid EH_{mn} and HE_{mn} waves. The resonance frequencies are determined by the edge conditions at the faces of the cylinder. Fig. 1 shows the four lowest modes of such a resonator, which is bounded by one electric and one magnetic wall. This approximates a cylinder with one face bound to a metallic surface.

The resonance frequencies of the unmagnetized ferrite can be calculated according to [12]. Fig. 2 shows the

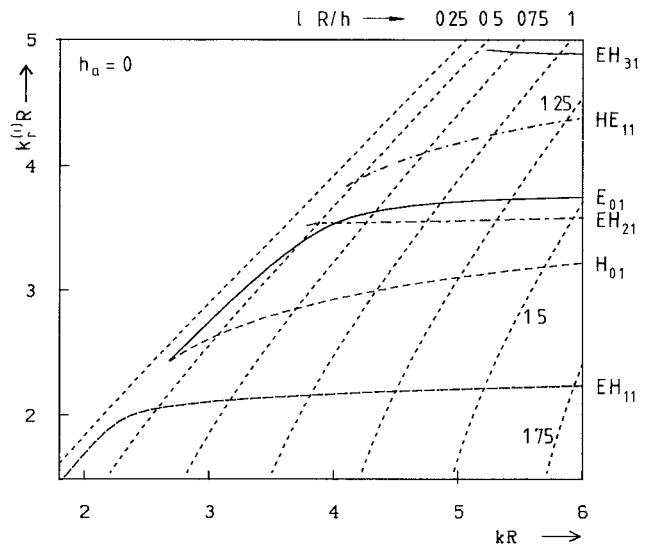

Fig. 2. Mode chart to determine resonant frequencies of the isotropic dielectric cylinder ($\epsilon_r = 12.5$; μ_f see Fig. 4).

normalized radial wavenumber $k_r^{(i)}R$ in the ferrite cylinder versus the wavenumber $kR = k_0\sqrt{\mu_z \epsilon_r}R$ in the ferrite. In a closed circular waveguide, this wavenumber would be represented as a horizontal line, which cuts the ordinate at the zeros of the Bessel function (H waves) or its derivative (E waves). All wave types except the EH_{11} have a cutoff frequency, below which the axial propagation constant becomes imaginary.

The curves in Fig. 2 have been calculated by [12], which has been generalized to $\mu_z \neq 1$. It is the solution of

$$U \cdot V - W^2 = 0 \tag{4}$$

with

$$U = \frac{1}{x}J_n'(x) + \frac{1}{\epsilon_r y}\frac{K_n'(y)}{K_n(y)}J_n(x)$$

$$V = \frac{1}{x}J_n'(x) + \frac{1}{\mu_z y}\frac{K_n'(y)}{K_n(y)}J_n(x)$$

$$W = n\frac{\beta}{k}\left(\frac{1}{x^2} + \frac{1}{y^2}\right)J_n^2(x) \tag{5}$$

where $J_n(x)$ and $J_n'(x)$ are the Bessel function of the first kind, nth order, and its derivative; $K_n(y)$ and $K_n'(y)$ are the modified Hankel function, nth order, and its derivative; $k = k_0\sqrt{\mu_z \epsilon_r}$ with $k_0 = \omega\sqrt{\mu_0 \epsilon_0}$; $x = k_r^{(i)}R$; $\beta R = \sqrt{(kR)^2 - x^2}$; and $y = k_r^{(a)}R = \sqrt{(\beta R)^2 - (k_0 R)^2}$.

The second family of curves is given by the height-dependent index l of the resonator mode from the condition

$$\beta h = \sqrt{(kR)^2 - \left(k_r^{(i)}R\right)^2}\,\frac{h}{R} = \pi l. \tag{6}$$

These are hyperbolas with the parameter lR/h. The abscissa value of the intersection point yields the normalized wavenumber kR. It must be denormalized to achieve the

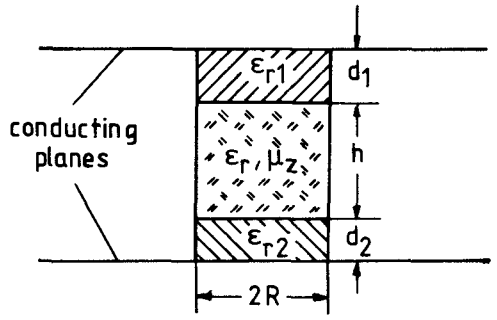

Fig. 3. Resonator with dielectric spacers between two infinite metallic walls.

resonant frequency

$$f = \frac{kR}{2\pi\sqrt{\epsilon_r \mu_z}\sqrt{\epsilon_0 \mu_0}\,R}. \tag{7}$$

The value l is only known exactly if the ferrite rod is placed between two electric or magnetic walls (integer l) or between an electric and a magnetic one (half-integer l). An open end of the resonator is only approximately a magnetic wall, as the fields extend to the space beyond the surface. Whereas this is generally a good assumption for E or EH waves in the ferrite rod, it may be insufficient for H and HE waves, which are more strongly affected by the imperfect magnetic wall boundary because of their higher field wave impedance.

To achieve more exact results in this case, the method of Itoh and Rudokas [11], [12] can be employed. To analyze the structure of Fig. 3, where the ferrite is mounted with dielectric spacers of thicknesses d_1 and d_2 and relative dielectric constants ϵ_{r1} and ϵ_{r2} between two electric walls, the transversal field components are matched at the plane boundaries. The waves in the dielectric spacers are assumed evanescent and purely transversal; hence the axial components are not matched. This makes an error of the order of 2 percent [12] for the H_{0nl} and HE_{mnl} resonance frequencies. The approximation is better the smaller the gaps d_1 and d_2 are. The resulting condition, which is generalized from [12, eq. (4.107)], for H and HE modes is

$$\beta h = \pi l = \pi p + \arctan\left(\frac{\mu_z \alpha_1}{\beta}\coth(\alpha_1 d_1)\right) + \arctan\left(\frac{\mu_z \alpha_2}{\beta}\coth(\alpha_2 d_2)\right) \qquad (p = 0,1,2,\ldots) \tag{8}$$

and for E and EH modes is

$$\beta h = \pi l = \pi p - \arctan\left(\frac{\epsilon_{r1}\beta}{\epsilon_r \alpha_1}\coth(\alpha_1 d_1)\right) - \arctan\left(\frac{\epsilon_{r2}\beta}{\epsilon_r \alpha_2}\coth(\alpha_2 d_2)\right) \qquad (p = 1,2,3,\ldots) \tag{9}$$

where

$$\beta = \frac{1}{R}\sqrt{(kR)^2 - \left(k_r^{(i)}R\right)^2}$$

$$\alpha_{1,2} = \frac{1}{R}\sqrt{\left(k_r^{(i)}R\right)^2 - \frac{\epsilon_{r1,2}}{\mu_z \epsilon_r}(kR)^2}. \tag{10}$$

If one of the electric walls is replaced by a magnetic wall (e.g. the center symmetry plane in an E-plane circulator), the corresponding coth function in (8) and (9) has to be replaced by the tanh function. Equations (8) and (9) with (10) are implicit relationships between (kR) and $(k_r^{(i)}R)$. Their locus curves can replace the hyperbolas of (6) for the second resonance condition. They depend on the parameters h/R, $d_{1,2}/R$, $\epsilon_{r1,2}/(\mu_z \epsilon_r)$, and p. Unfortunately (8) and (9) cannot be solved analytically for kR or $(k_r^{(i)}R)$.

In practice, however, this need not be done. Utilizing a simple pocket calculator and the diagram Fig. 2, the resonant frequencies can be found by an iterative procedure:

1) Assume an initial value for l (e.g. using the magnetic wall condition).
2) Interpolate the hyperbola with the parameter lR/h in Fig. 2.
3) Look up the coordinates $(kR, x = k_r^{(i)}R)$ of the intersection of this hyperbola with the dispersion curve of the mode under investigation.
4) Calculate the value of l resulting from (8) or (9), respectively.
5) Compare this value of l with the former one. If there is still a considerable deviation, go back to point 2; otherwise the correct resonance frequency has been found.

Usually, after the second iteration the frequency is already settled. This can be checked in a third iteration step.

According to [12], the accuracy of this method (i.e., the simultaneous solution of (4) and (8)/(9)) is within 6 percent for the H_{01l} mode. For the E and EH modes it can be expected to be better. The accuracy is also greatly improved if electric walls are not too far away from the ferrite surfaces. (If they contact the ferrite, the solution is exact!) This is the case for most junction circulators.

At this point, some remarks must be made concerning the material parameters ϵ_r and μ_z. The diagram in Fig. 2 and all following diagrams are calculated for $\epsilon_r = 12.5$, a usual value for microwave ferrites. Slight deviations from this value (say $10 \cdots 15$) do not affect the shape of the curves significantly, so they can still be used. Obviously, the correct value of ϵ_r must be used for the denormalization after (7). The same consideration holds for μ_z, which is slightly lower than 1. As this value is a function of $w = \omega/\omega_m$ (2), we must fix a relation between the operating frequency and the saturation magnetization. For the diagrams given here this has been chosen to make the frequency for which $kR = 1.84$ (the E_{110} resonance of a resonator with magnetic wall, which is a sort of lower limit for all height-dependent resonance frequencies) correspond to the normalized frequency $w = 1.3$. This is a common choice for the lower limit of the operating bandwidth to

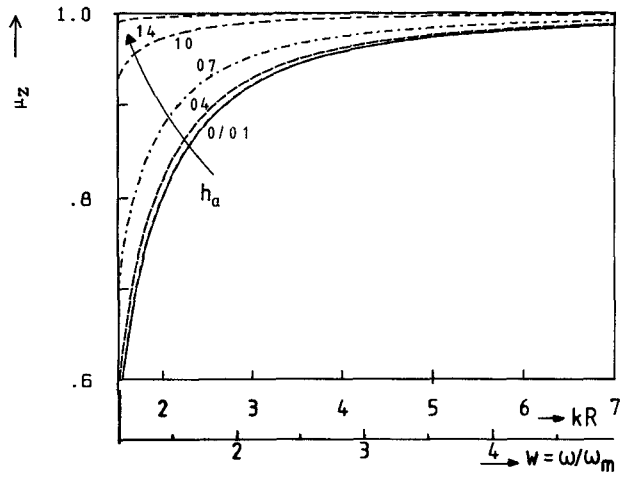

Fig. 4. μ_z element of the permeability tensor versus normalized frequency.

ensure that low-field loss is negligible. The element μ_z, which is needed for calculating the frequency by (7), is shown in Fig. 4 versus frequency for various magnetic fields. To facilitate the use of the mode charts, in addition to $w = \omega/\omega_m$ also $kR = (1.84/1.3)(\omega/\omega_m)$ has been given on the abscissa.

IV. Resonance Frequencies of the Magnetized Ferrite

The procedure for calculating the eigenfrequencies with the magnetized ferrite can be taken from [4] or [13] with the modifications for $\mu_z \neq 1$ added. For the sake of brevity, only the final results of this tedious analysis shall be given. Inside the ferrite, the longitudinal electric field E_z of a wave traveling in the z direction with the propagating constant β must obey one of the differential equations

$$\left(\nabla_t^2 + k_{t1}^2\right)E_z = 0 \quad \text{or} \quad \left(\nabla_t^2 + k_{t2}^2\right)E_z = 0 \tag{11}$$

with ∇_t the transversal components of the nabla operator, and

$$k_{t1,2}^2 = \frac{1}{2}\left[k^2\left(\frac{\mu_{\text{eff}}}{\mu_z}+1\right) - \beta^2\left(\frac{\mu_z}{\mu}+1\right)\right] \pm \frac{1}{2}\sqrt{\left[k^2\left(\frac{\mu_{\text{eff}}}{\mu_z}-1\right)+\beta^2\left(\frac{\mu_z}{\mu}-1\right)\right]^2 + \left(2\beta k\frac{\kappa}{\mu}\right)^2}$$

$$\mu_{\text{eff}} = \frac{\mu^2-\kappa^2}{\mu} \qquad k = \omega\sqrt{\mu_z \epsilon_r \mu_0 \epsilon_0}\,. \tag{12}$$

The solutions corresponding to k_{t1} and k_{t2} being called E_{z1} and E_{z2}, the other field components can be expressed by

$$H_{z1,2} = jB_{z1,2}E_{z1,2}$$

$$\vec{E}_{t1,2} = -jA_{1,2}\nabla_t E_{z1,2} + B_{1,2}\nabla_t \times E_{z1,2}\vec{e}_z$$

$$\vec{H}_{t1,2} = C_{1,2}\nabla_t E_{z1,2} + jD_{1,2}\nabla_t \times E_{z1,2}\vec{e}_z \tag{13}$$

with the coefficients

$$B_{z1,2} = Y\frac{\frac{\kappa}{\mu}\beta k}{k^2 - \frac{\mu_z}{\mu}\beta^2 - k_{t1,2}^2} = Y\frac{k^2\frac{\mu_{\text{eff}}}{\mu_z} - \beta^2 - k_{t1,2}^2}{\frac{\kappa}{\mu}\beta k}$$

$$A_{1,2} = \frac{\beta}{k_{t1,2}^2} \qquad B_{1,2} = \frac{kB_{z1,2}Z}{k_{t1,2}^2}$$

$$C_{1,2} = \frac{\mu_z Y}{\kappa k}\left(\frac{k^2\frac{\mu}{\mu_z} - \beta^2}{k_{t1,2}^2} - 1\right) \qquad D_{1,2} = \frac{kY}{k_{t1,2}^2}$$

$$Z = \frac{1}{Y} = \sqrt{\frac{\mu_z\mu_0}{\epsilon_r\epsilon_0}}\,. \tag{14}$$

In the limit of $\kappa \to 0$ or $\beta \to 0$, the solution with k_{t1} approaches an E wave, and that with k_{t2} an H wave. The actual field in the ferrite is now expressed as a superposition of these two solutions. This means for E_z:

$$E_z^{(i)} = \left\{a_n \underline{J}_n(k_{t1}r) + b_n \underline{J}_n(k_{t2}r)\right\} e^{jn\phi}e^{-j\beta z}. \tag{15}$$

$\underline{J}_n(x)$ is the Bessel function generalized to complex arguments ($\underline{J}_n(jx) = j^n I_n(x)$). The other field components are calculated by (13).

For the external region, decaying TE and TM waves with modified Hankel functions are superposed. The boundary conditions at $r = R$ yield the following characteristic equation:

$$U_1V_2 - U_2V_1 = 0 \tag{16}$$

with

$$U_{1,2} = \underline{J}_n(k_{t1,2}R)\cdot\left[\frac{n}{R}\left(A_{1,2}+\frac{\beta}{g^2}\right) - B_{z1,2}Z_0\frac{k_0}{g}\frac{K_n'(gR)}{K_n(gR)}\right] - k_{t1,2}B_{1,2}\underline{J}_n'(k_{t1,2}R)$$

$$V_{1,2} = \underline{J}_n(k_{t1,2}R)\cdot\left[\frac{n}{R}\left(C_{1,2}+\frac{\beta}{g^2}B_{z1,2}\right)Z_0 - \frac{k_0}{g}\frac{K_n'(gR)}{K_n(gR)}\right] - k_{t1,2}D_{1,2}\underline{J}_n'(k_{t1,2}R)$$

$$g = \sqrt{\beta^2 - k_0^2} \qquad Z_0 = \frac{1}{Y_0} = \sqrt{\frac{\mu_0}{\epsilon_0}} \qquad k_0 = \omega\sqrt{\mu_0\epsilon_0}\,. \tag{17}$$

This equation replaces (4) in the anisotropic case.

Equation (16) with (17) has been solved numerically. The elements of the permeability tensor are calculated by (2). For a fixed value of kR, the normalized propagating constant βR is evaluated. If the ferrite radius is stepped monotonically, a good starting value for βR can be extrapolated from the calculations already done, so that the zero is found very fast. In Figs. 5 to 8 the result is shown for the EH_{11l}, the HE_{01l}, the EH_{01l}, and the EH_{21l} mode. The first equation of (14) reveals that for $B_{z1,2} \neq 0$ or infinity there are always E_z as well as H_z components; even the modes with the azimuthal index 0 are of hybrid character if the ferrite is magnetized. As in Fig. 2, instead of βR the radial wavenumber in the ferrite $k_r^{(i)}R$ is given as the ordinate,

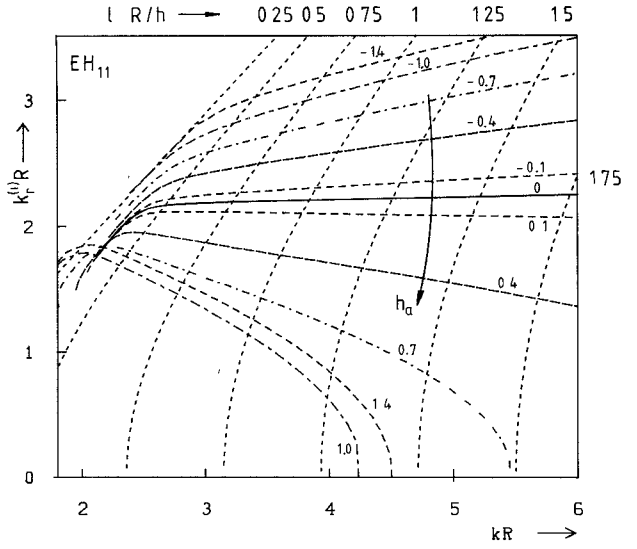

Fig. 5. Mode chart to determine the EH_{11l} resonant frequency of the magnetized ferrite cylinder ($\epsilon_r = 12.5$; μ_f see Fig. 4).

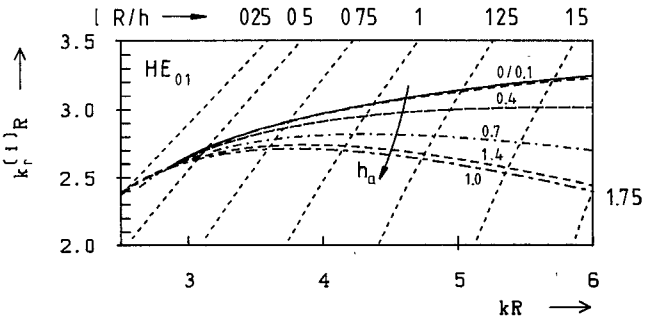

Fig. 6. Mode chart to determine the HE_{01l} resonant frequency of the magnetized ferrite cylinder ($\epsilon_r = 12.5$; μ_f see Fig. 4).

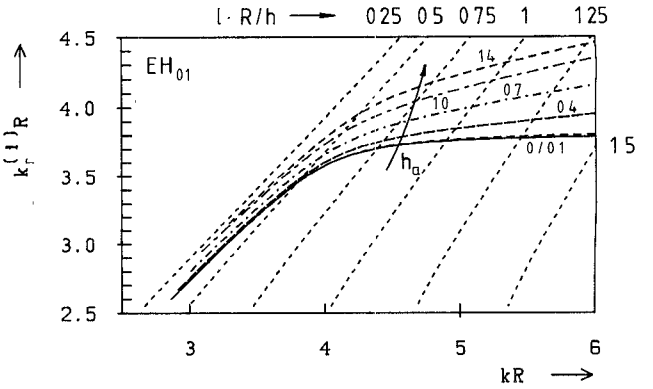

Fig. 7. Mode chart to determine the EH_{01l} resonant frequency of the magnetized ferrite cylinder ($\epsilon_r = 12.5$; μ_f see Fig. 4).

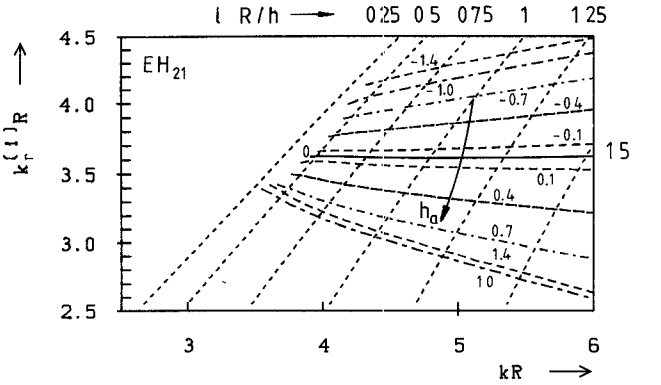

Fig. 8. Mode chart to determine the EH_{21l} resonant frequency of the magnetized ferrite cylinder ($\epsilon_r = 12.5$; μ_f see Fig. 4).

which is defined as in the isotropic case as $k_r^{(l)} = \sqrt{k^2 - \beta^2} = \sqrt{\mu_z \epsilon_r k_0^2 - \beta^2}$. In contrast to the isotropic case, this is a fictitious number, because physically there is a superposition of fields with both transversal wavenumbers k_{t1} and k_{t2} in the ferrite. In certain regions one of these becomes imaginary; the corresponding part of the field is then guided at the ferrite–air boundary and decays aperiodically in both directions (edge-guided modes). In height-independent structures (stripline circulators) there are even modes with all the field guided in this way (for $\mu_{\text{eff}} \lessapprox 0$). There is, however, no necessity to treat them in a special way, because resonance frequencies vary continuously at the transition from radially periodic to aperiodic modes. This is also accentuated by a recently presented microstrip circulator, whose operating bandwidth covers this transition [14]. In Figs. 5 to 8 the eigenvalues with negative order n are shown with negative h_a. In fact, inverting the bias field ($\kappa \to -\kappa$) is equivalent to changing the direction of polarization. For the angle-dependent modes, frequency splitting strongly increases with the field in the unsaturated region, while it remains constant or even decreases at higher fields $h_a > 1$ to become zero again for $h_a \to \infty$. It is worth noting that the lower split frequency, which decreases with rising h_a for low bias fields, rises again for $h_a \gtrapprox 1$. Due to the change in μ_{eff} the angle-independent modes HE_{01} and EH_{01} also change their resonance frequencies, namely in opposite directions. Relative frequency splitting is largest at small lR/h; i.e., the disks should not be too flat. Furthermore, this means a larger distance between the $E_{\pm 11l}$ and those with a higher order angle dependence, so that the latter cannot cause unwanted resonances in the operating bandwidth. Splitting of about 40 percent can be achieved.

The diagrams in Figs. 5 to 8 have been used in [15] to identify resonances of the S-parameter eigenvalues measured in waveguide circulators. For a ferrite rod reaching from one circulator wall to the other, the predictions were exact within the limits of the graphical readout. This is not surprising, because the axial index is an integer and exactly known. The resonant frequencies of the height-independent modes are determined by the lateral boundaries of the junction. They cannot be found by only analyzing the ferrite cylinder, because the RF fields extend to infinity. But as this is only a two-dimensional problem, the exact analysis is not too difficult. It has been done by the method of Davies [16].

For partial-height ferrite resonators, there is the problem of finding the correct axial index. It has been solved in the manner described in Section III for the dielectric resonator. As the hybrid character of the ferrite modes is more accentuated, the error in the resonance frequencies

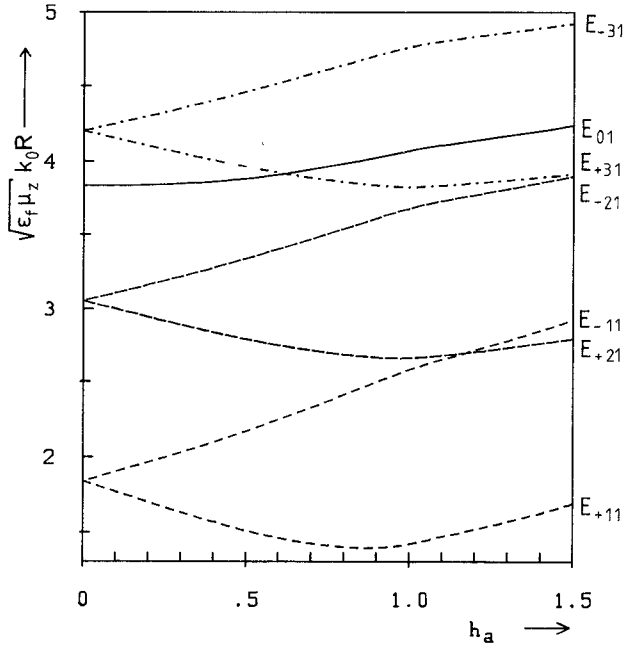

Fig. 9. Mode chart to determine the height-independent modes of a ferrite cylinder with magnetic wall.

can be up to 10 percent for the HE_{01l} modes; for the EH_{mnl} modes some 4 percent are reached. This is sufficient for the identification of spurious resonances. For more exact calculations of circulators including spurious resonator modes, very extensive three-dimensional calculations must be performed, as described in [6] and [17]–[19].

For completeness, a diagram for the height-independent resonator modes will also be given; these modes play the essential role in stripline and microstrip circulators. As height-independent modes in radially open structures always radiate, there must be a conducting radial boundary, in the simplest case a magnetic wall around the ferrite. Neglecting fringing fields, it is defined by the periphery of the metallization above the ferrite. The solution is simple and has been given e.g. in [1] versus the magnetic splitting κ/μ. As this value also depends on frequency, this chart is not very helpful for the design. The diagram of Fig. 9 shows instead the normalized resonance frequencies versus the external magnetic bias field h_a. The achievable frequency splitting is generally larger than that for height-dependent modes, because there are no axial magnetic RF components which do not contribute to nonreciprocity.

Above saturation ($h_a \gtrapprox 1$) the E_{+11} and the E_{-21} modes have nearly the same resonant frequency. Both modes are bound to the same eigenexcitation, so that one of them can take over the role of the other. This is the case for the "continuous tracking" circulator in [20].

V. Conclusions

Mode charts have been given for the transversal wavenumber in ferrite rods versus the material wavenumber of the demagnetized ferrite. If a piece of this rod is terminated by conducting walls, the exact frequencies of the resonator installed in this way can be found by a simple graphical procedure. If one or both ends of the ferrite are left open, a modified procedure leads to approximate values for the frequencies, which may deviate from the true values by up to 10 percent. The diagrams are intended to estimate the frequencies of wanted and unwanted resonances in junction circulators without tedious calculations.

Acknowledgment

The author wishes to thank U. Goebel for helpful discussions.

References

[1] H. Bosma, "On stripline circulation at UHF," *IEEE Trans. Microwave Theory Tech.*, vol. MTT-12, pp. 61–72, 1964.

[2] J. Helszajn and J. Sharp, "Resonant frequencies, Q-factors, and susceptance slope parameter of waveguide circulators using weakly magnetized open resonators," *IEEE Trans. Microwave Theory Tech.*, vol. MTT-31, pp.434–441, 1983.

[3] J. Helszajn and J. Sharp, "Dielectric and permeability effects in HE_{111} open demagnetized ferrite resonators," *Proc. Inst. Elec. Eng.*, pt. H, vol. 133, pp. 271–276, 1986.

[4] H. D. Godtmann and W. Haas, "Magnetodynamic modes in axially magnetized ferrite rods between two parallel conducting sheets," *IEEE Trans. Microwave Theory Tech.*, vol. MTT-15, pp. 476–481, 1967.

[5] H. D. Godtmann, "Über elektromagnetische Eigenschwingungen offener kreiszylindrischer Resonatoren im Mikrowellen-Bereich," thesis TH Aachen, West Germany, 1966.

[6] W. Hauth, "Analysis of circular waveguide cavities with partial height ferrite insert," in *Proc. 11th European Microwave Conf.* (Amsterdam), 1981, pp. 383–388.

[7] W. Hauth, "Feldtheoretische Analyse von Verzweigungszirkulatoren mit parallel zur Verzweigungsebene geschichteten Medien," thesis TH Erlangen-Nürnberg, West Germany, 1982.

[8] D. Polder, "On the theory of ferromagnetic resonance," *Phil. Mag.*, vol. 40, pp. 99–115, 1949.

[9] J. J. Green and F. Sandy, "Microwave characterization of partially magnetized ferrites," *IEEE Trans. Microwave Theory Tech.*, vol. MTT-22, pp. 641–645, 1974.

[10] B. Hansson and G. Filipsson, "Microwave circulators in stripline and microstrip techniques," Rep. TR 7606, Chalmers University of Technology, Div. of Network Theory, Gothenburg, Sweden, 1976.

[11] T. Itoh and R. S. Rudokas, "New method for computing the resonant frequencies of dielectric resonators,"*IEEE Trans. Microwave Theory Tech.*, vol. MTT-25, pp. 52–54, 1977.

[12] D. Kajfez and P. Guillon, Eds., *Dielectric Resonators*, Dedham, MA; Artech House, 1986.

[13] I. Wolff, *Felder und Wellen in gyrotropen Mikrowellenstrukturen*, Vieweg, Braunschwieg, West Germany, 1973.

[14] E. Schlömann and R. E. Blight, "Broadband stripline circulator," in *IEEE MTT-S Int. Microwave Symp. Dig.* (Baltimore), 1986, pp. 739–742.

[15] C. Schieblich, "Theorie und Entwurf von Verzweigungs-Zirkulatoren," thesis TU Hamburg-Harburg, West Germany, 1987.

[16] J. B. Davies, "An analysis of the m-port symmetrical H-plane waveguide junction with central ferrite post," *IRE Trans. Microwave Theory Tech.*, vol. MTT-10, pp. 596–604, 1962.

[17] M. E. El-Shandwily, A. A. Kamal, and E. A. F. Abdallah, "General field theory treatment of E-plane waveguide junction circulators—Part II: Two disk ferrite configuration," *IEEE Trans. Microwave Theory Tech.*, vol. MTT-25, pp. 794–803, 1977.

[18] Y. Akaiwa, "A numerical analysis of H-plane Y-junction circulators with circular partial height ferrite post," *Trans. IECE Japan*, vol. E 61, pp. 609–617, 1978.

[19] R. J. Copplestone, "An exact three-dimensional field theory for a class of cyclic H-plane waveguide junctions," *IEEE Trans. Mi-*

crowave Theory Tech., vol. MTT-27, pp. 577–584, 1979.
[20] Y. S. Wu and F. J. Rosenbaum, "Wideband operation of microstrip circulators," *IEEE Trans. Microwave Theory Tech.*, vol. MTT-22, pp. 849–856, 1974.

✠

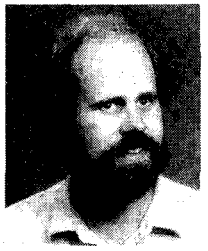

Christian Schieblich was born in Salzgitter, Germany, on January 1, 1954. He received the Dipl.-Ing. degree from the Technische Universität Braunschweig in 1979 and the Dr.-Ing. degree from the Technische Universität Hamburg–Harburg in 1987. His thesis dealt with the design of ferrite junction circulators.

From 1979 to 1983 he was assistant at the Institut für Hochfrequenztechnik at the Technische Universität Braunschweig and then at the Arbeitsbereich Hochfrequenztechnik at the Technische Universität Hamburg-Harburg, where he worked on ferrite components and various microwave and millimeter-wave finline applications. Since 1987 he has been with the CERN European Research Center in Geneva, where he works on RF systems for linear accelerators for elementary particles.